Liquid Encapsulation by Binary Collisions of Immiscible Liquid Drops

C. Planchette, G. Brenn*
Laboratoire de Physique des Matériaux Divisés et des Interfaces, Université Marne-la-Vallée
UMR 8108 du CNRS, 5 boulevard Descartes, 77454 Marne-la-Vallée cedex 2, France
Tel. +33 1 60 95 73 25, Fax. +33 1 60 95 72 97, Email carole.planchette@univ-mlv.fr
*Institute of Fluid Mechanics and Heat Transfer, Graz University of Technology
Inffeldgasse 25/F, 8010 Graz, Austria
Tel. +43 316 873-7341, Fax. +43 316 873-7356, Email brenn@fluidmech.tu-graz.ac.at

Abstract

In this paper, we present binary collisions of immiscible liquid drops as a promising and reliable process for encapsulating liquids in shells of other, immiscible liquids. Our current experimental approach describes the collision outcome according to relevant parameters. Depending on the drop size and the relative velocity, the impact parameter and liquid viscosity, density and surface tension, we observe that either the full drop of encapsulating liquid spreads around the encapsulated one, or part of it separates, while the rest remains attached. We show that the viscosities of the two liquids do not have equal importance for the stability limit of the process, especially for head-on collisions. For separated drops, the thickness of the remaining liquid shell was also investigated and turns out to be independent of both liquid viscosities and relative velocity. As a consequence, we can accurately adjust the thickness of the coating layer by simply tuning the impact parameter of the collision. An interpretation of this behavior based on a geometric argument is proposed.

Introduction

Collisions of drops of the same liquid are of high interest for meteorological and spray applications. Further to this significance, drop collisions may be essential for production processes in some life sciences, such as the coating of a liquid core by another immiscible liquid. The aim of our work is to study collisions of immiscible liquid drops as a promising and reliable way to achieve drop encapsulation with a tunable shell thickness. The interactions most often occur with pairs of drops; collisions of three or more drops are much less probable. Since binary drop collisions affect the spectra of both the drop size and the drop velocity, much effort has been invested in characterizing this process. The large computational expenditure needed for detailed simulations of free-surface flows justifies the use of experimental approaches [1-7].

For equal-sized drops, the four possible regimes (coalescence, bouncing, stretching separation and reflexive separation) are represented using an X–We nomogram (*see* Fig. 1). $X=x/D$ is the normalized impact parameter, with the impact parameter x (*see* Fig. 2), $We=U^2D\rho/\sigma$ is the drop Weber number, with the liquid density ρ and surface tension σ, the relative velocity U and diameter D of the drops.

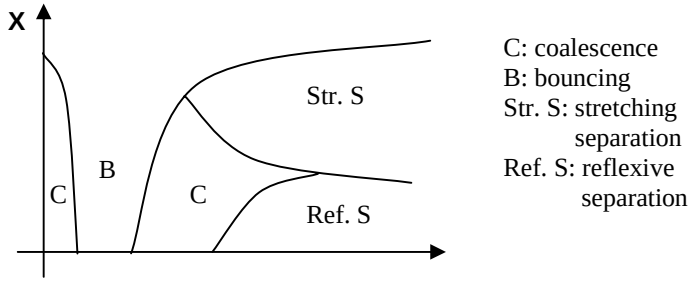

Figure 1. Different regimes of binary drop collisions as functions of X and We.

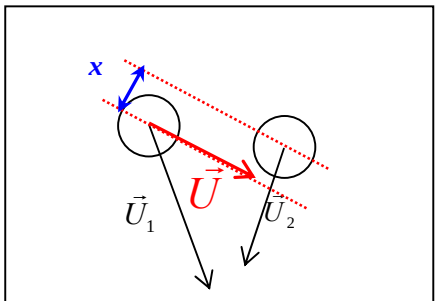

Figure 2. Definition of the impact parameter x.

*Corresponding author

Most of the developed models do not take into account the viscosity, but predict relatively well the experimental results for given test liquid and background gas conditions. Drop collisions involving different liquids are only sparsely investigated [8-10]. At moderate *We*, and for miscible liquids, the observed regimes are similar to the ones of single liquid drop collisions: bouncing, coalescence, and stretching and reflexive separation.

Considering that the process relies on the conversion of the initial kinetic energy of the two drops into surface energy plus an eventual rotation component and losses due to viscous dissipation, we vary the sizes and relative velocities of the drops, the impact parameter, and the density, viscosity, surface tension and interfacial tension of the pairs of liquids. We first present the stability behaviour of the collisions for a given pair of liquids as a function of the relative velocity and the impact parameter. From these experiments we get nomograms as in Fig. 1, which indicate the different regimes by zones of bouncing, drop coalescence and separation. It is interesting to note that the mechanism of reflexive separation observed in head-on and near-head-on collisions of drops from miscible liquids does not exist for immiscible liquids. To our knowledge, the process that takes place instead has not been identified in the literature so far. We will refer to it as the "crossing separation" mechanism. Varying the viscosity of the two liquids independently from the other properties, we evaluated the importance of viscous dissipation in both encapsulated and encapsulating drops, as well as its effect on stability limits. Another focus of our interest is on the outcome from the drop collisions, in particular on the sizes of the drops after the collision and the volume of the liquid coating on the inner drop. This latter volume is measured and exhibits a stepwise evolution with increasing impact parameter of the collision. It is of great interest to note that this evolution is affected neither by the relative velocity, nor by the liquid viscosities and provides us a simple and reliable way of tuning the shell thickness of the encapsulated drop. Our interpretation of this result is presented in the last section of this paper.

Materials and Methods

- Experimental Set-up

To realise binary collisions of immiscible liquid drops in a controlled way, we use two drop generators producing continuous streams of monodisperse drops of varying sizes [12], as shown in Fig. 3. The drop trajectories are adjusted with an accuracy of ±2µm, allowing us to vary their relative velocity U at impact, as well as the non-dimensional impact parameter X. An ultra-fast flash, synchronized with the drop generators, and a Sensicam fast shutter video camera produce images of the collisions. From those pictures we determine the sizes of the drops before and after the collision, and deduce the drop velocities and the impact parameter.

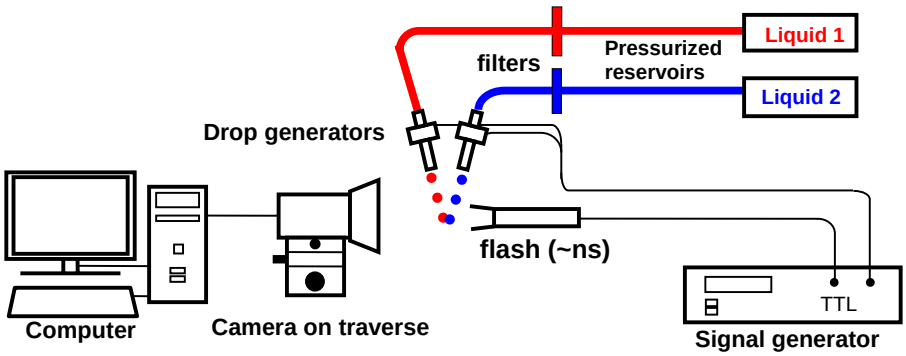

Figure 3. Experimental set-up

- Liquids

In order to encapsulate a liquid core in a shell of another, immiscible one, we selected aqueous glycerol solutions and a group of oils. The influence of the liquid viscosity on the outcome of the encapsulation process is investigated using different concentrations of glycerol as well as two different silicon oils. Influences of other liquid properties, such as density, surface tension and interfacial tension, are still under investigation.

Because of their high surface tension, the glycerol solutions are very sensitive to surface pollution. They are therefore prepared with pure water on the day of the experiments. Their concentration is given in weight percent. Density and surface tension of each liquid from both phases, as well as the interfacial tension of the pair of liquids were measured. The accuracy of density measurements is ±0.2 $kg \cdot m^{-3}$. Surface tension is determined with the pending drop method using a tensiometer Lauda TVT2 at a maximum uncertainty ±0.4 $mN \cdot m^{-1}$. The viscosity of glycerol solutions is taken from reference [11]. The oils were purchased from Carl Roth Ltd. under the names of silicon oil M3 (SO M3) and M5 (SO M5) with kinematic viscosities of 3 mm^2/s and 5 mm^2/s, respectively. A summary of the

liquid properties is given in Table 1. It is important to note that this choice of liquids allows us to realize a full closed encapsulation. From the surface and interfacial tension values we conclude that the oils totally wet the glycerol solutions, which ensures full coating of the aqueous phases by the oils.

Table 1. Liquid properties at 20 °C.

Liquid	Density [kg·m^{-3}]	Dynamic viscosity [mPa·s]	Surface tension [mN·m^{-1}]	Interfacial tension [mN·m^{-1}]	
				with SO M3	with SO M5
Glycerol 20%	1047.9	1.76	70.7	37.7	
Glycerol 30%	1072.9	2.50	70.3	36.7	
Glycerol 40%	1098.8	3.72	69.5	34.9	
Glycerol 50%	1126.0	6.00	68.6	34.8	34.3
Glycerol 55%	1139.0	Extrapolated 7.8	68.1	33.8	
SO M3	892.2	2.677*	19*	* values from Carl Roth datasheet.	
SO M5	913.4	4.567*	19*		

Results and Discussion

We first worked on the regimes of the encapsulation process for a given pair of liquids, varying both the impact parameter of the collision and the relative velocity of the drops. Using *SO M3* and a solution of glycerol at 50%, we observed the two following outcomes: either the entire oil drop remains spread around the aqueous one (coalescence), or part of it is expelled, leaving a rest as the coating (separation). A picture of total coalescence is shown in Fig. 4. Concerning the partial coalescence, we identified two independent mechanisms: for low impact parameters, the aqueous drop goes through the oil, resulting in a separation where both drops keep their initial relative direction (Fig. 5). It is interesting to note that this "crossing separation" (so termed by us) is very different from the reflexive separation observed in head-on collisions of drops of miscible liquids. In reflexive separation, the relative direction of the drops is exchanged. The second mechanism leading to separation of immiscible liquid drops is observed for high impact parameter and corresponds to the stretching separation (Fig. 6). Immiscible as well as miscible liquids are stretched by the inertia of the drops, resulting in elongation of the connecting liquid bridge until its break-up.

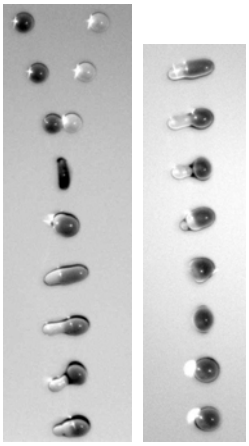

Figure 4. Coalescence of a glycerol solution drop at 50% (dark) and a SO M3 drop (bright). D=230 µm, U=2.30m/s, X=0.03.

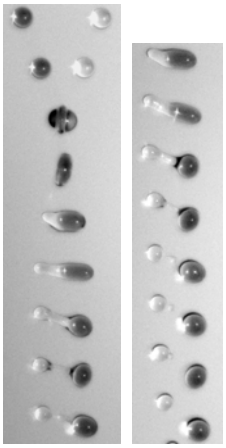

Figure 5. Crossing separation of a glycerol solution at 50% (dark) and a SO M3 (bright) drops. D=210 µm, U=2.75m/s, X=0.03.

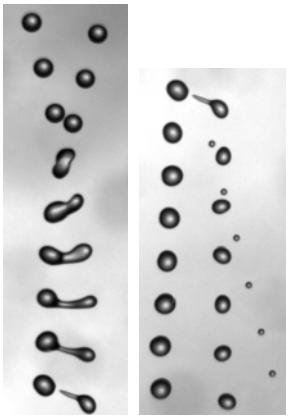

Figure 6. Stretching separation between a drop of glycerol solution at 50% (right upstream and left downstream) and an SO M3 drop (left upstream). D=190 µm, U=2.26m/s, X=0.49.

The stability limit against stretching separation is located at high impact parameter values and corresponds to the line A-B in Fig. 7. At zero impact parameter we can define the maximum relative velocity U_0 for stability regarding the crossing separation. It is interesting to note that the velocity can be increased over U_0, keeping a coalescence regime (see line C-B in Fig. 7). This stability is due to the non-zero impact parameter which allows a rotation of the merged drop around its gravity center. For $U > U_0$, this angular momentum stores a part of the excess kinetic energy. This effect, however, is limited: separation occurs again on the right of line B-C of Fig. 7.

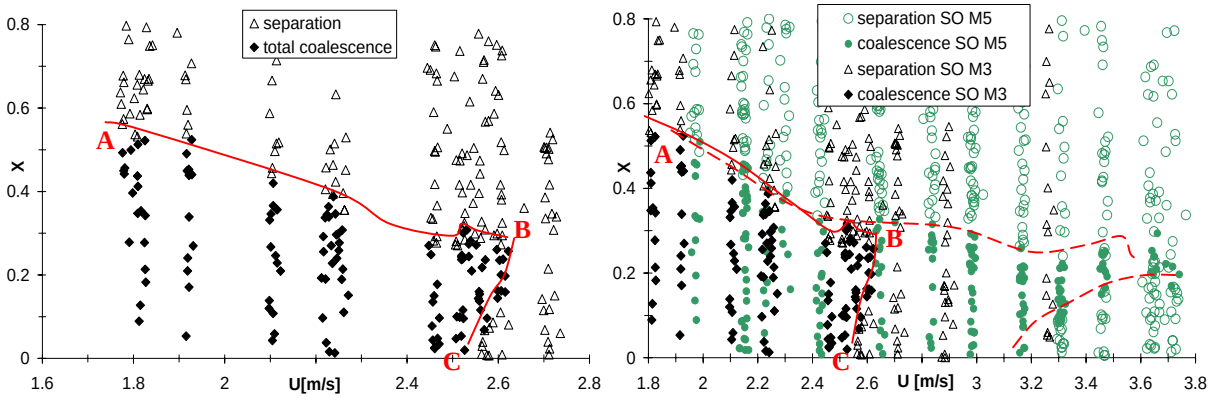

Figure 7. Left: nomogram representing the stability behavior of binary collisions of equal-sized drops. Liquids: glycerol solution at 50% and SO M3. Drop sizes: D=192µm ±4%. Right: nomogram obtained with the glycerol solution at 50% and SO M5. The "◆" and "Δ" refer to the same experiment with SO M3. D = 200µm ±10%.

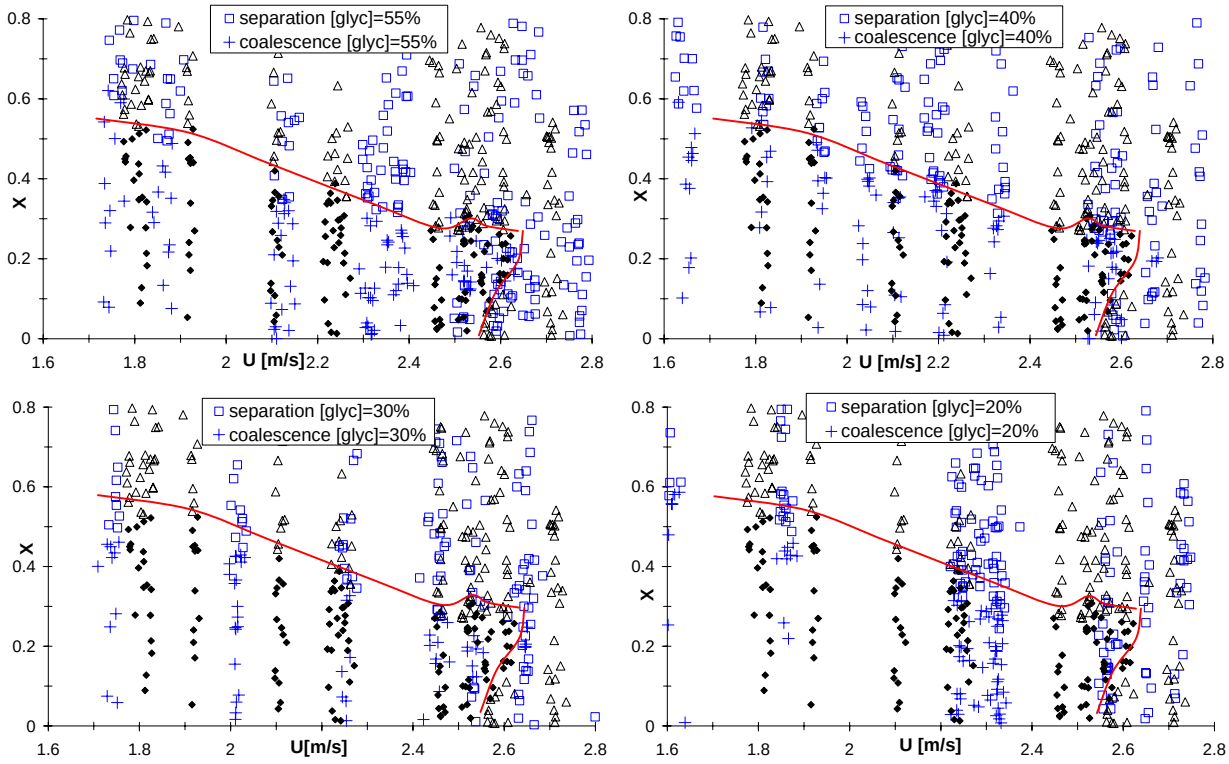

Figure 8. Nomograms obtained with SO M3 and glycerol solutions at 55%, 40%, 30% and 20% in weight. The "◆" and "Δ" refer to a glycerol concentration of 50%. The drops are equal-sized with D = 200µm ±10%.

To investigate the influence of viscous dissipation on the limits of total coalescence, we repeated the previous experiments with the same drop sizes for different pairs of liquids. First, we kept the SO M3 and varied the concentration of the glycerol solution, resulting in a change of the aqueous phase viscosity, independent from the other parameters. The results are presented in Fig. 8. In the next experiments we varied the viscosity of the encapsulating phase. Densities and surface tensions, as well as the interfacial tensions against the glycerol solution at 50 %, are almost constant for the two silicon oils. The nomogram obtained with SO M5 can be compared to the one for SO M3 in Fig. 7.

With the encapsulated phase viscosities between 2.5 mPa·s and 7.8 mPa·s, no significant variations in stability limits could be measured. For the glycerol solution at 20% (viscosity 1.7 mPa·s), the stability limit against crossing

separation may be slightly shifted to lower velocities ($2.35<U_0<2.55$m/s instead of 2.55m/s for all other concentrations). The stretching separation limit is not affected. In contrast, increasing the viscosity of the encapsulating phase leads to a significant shift of the crossing separation stability limit: $U_0>3.2$ m/s for SO M5 instead of 2.55m/s for SO M3. The stretching separation limit is almost unchanged. It is interesting to note that the asymmetry of the process is reflected by this result, i.e., by the fact that U_0 is independent of the encapsulated liquid viscosity, but varies with the viscosity of the encapsulating one. For zero impact parameter we can neglect the rotational energy and consider that the initial kinetic and surface energies of the two drops are dissipated by viscous losses. By this collision, the drops are distorted. The surface tension difference allows the oil to spread around the glycerol and encapsulate it. The mean flows are located in a thin film from the encapsulating drop spreading around the aqueous drop. Observing head-on collisions at different relative velocities, we notice that the time needed for the oil to arrive on the other side of the glycerol and generate a closed shell is almost constant: for U=2.23m/s, t=813μs; for U=2.463m/s, t=806μs; for U=2.60m/s, t=844μs; and for U=2.76m/s, t=833μs. Assuming that the spreading velocity of the oil U_{Spread} (in the θ direction of a spherical coordinate system) is not affected by the relative velocity of the drops, the dissipation associated to this flow is independent of U and can be written as

$E_{visc} \approx \int_t dt \int_{V_{oil}} \mu_o \left(r \frac{\partial (v_\theta / r)}{\partial r} \right)^2 dV \propto A \cdot \mu_o$, where A is a constant, μ_o the oil viscosity, $r\partial(v_\theta/r) / \partial r \sim U_{spread} / h$, and h is the thickness of the coating layer. This view is in good agreement with the experimental results: U_0 (SO M3)=2.55m/s, U_0 (SO M5)=3.25m/s, which leads to a kinetic energy ratio of 0.61. The viscosity ratio is 2.677/4.567=0.59.

For off-center collisions with stretching separation we focused on the volume of the oil shell remaining on the aqueous drop. This latter volume ΔV_c is determined as the difference between the volumes of the drops of the coating liquid upstream (V_0) and downstream from the impact point. Its non-dimensional form is defined as $\varphi = \Delta V_c / V_0$. In cases of permanent coalescence of the two drops, $\varphi = 1$. For $X<0.5$, the existence of a stepwise evolution of φ as well as the position of the corresponding threshold depends on U. As it can easily be seen in Fig. 9, for a given U with $U(A)< U < U_0$ (*see* Fig. 7) there is a single threshold which decreases with increasing U. For $U_0<U<U(B)$ (*see* Fig. 7), two thresholds can be seen, corresponding to the two stability limits. If U is further increased, i.e., for $U>U(B)$ in Fig. 7, these two limits overlap and a threshold does not exist any more. It is interesting to note that, for $X>0.5$, the volume ratio φ is independent of U (Fig. 9). Experiments using different pairs of liquids show that, for $X>0.5$, φ is also independent of both the encapsulated and the encapsulating liquid viscosities (*see* Fig. 10).

Comparing the results of Figs. 9 and 10 we see that, if we take into account the error bars (not represented in Fig. 10 for clarity), all points collapse on one line. The dashed lines of Figs. 9 and 10 ("pure geometric capture") assume that the quantity of oil coating on the aqueous drop corresponds to the interacting volume defined in Fig. 11. The experimental volumes, however, are slightly smaller. This may be due to the fact that, while the drops come into

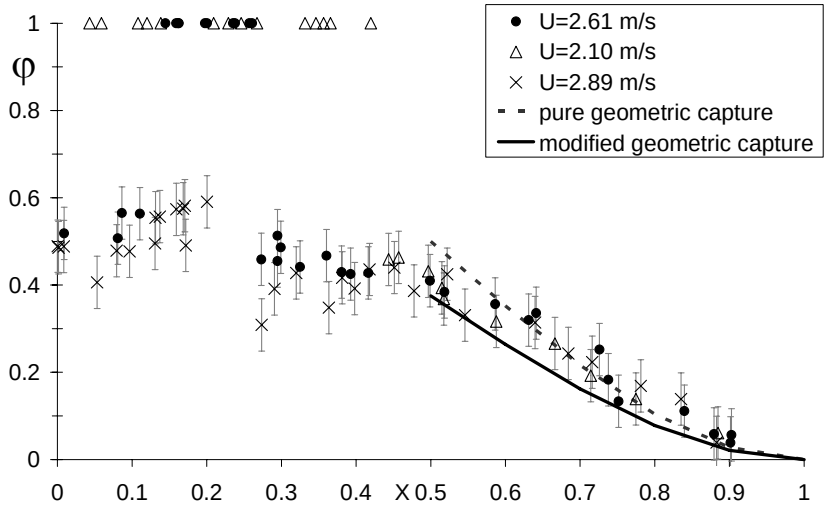

Figure 9. Evolution of φ with X. For U= 2.61 m/s "•" (between B and C in Fig. 7), U=2.10 m/s "Δ" (left of C in Fig. 7), and U= 2.9 m/s "×" (right of B in Fig. 7). Liquids: SO M3, glycerol solution at 50%. D=200 μm ±10%.

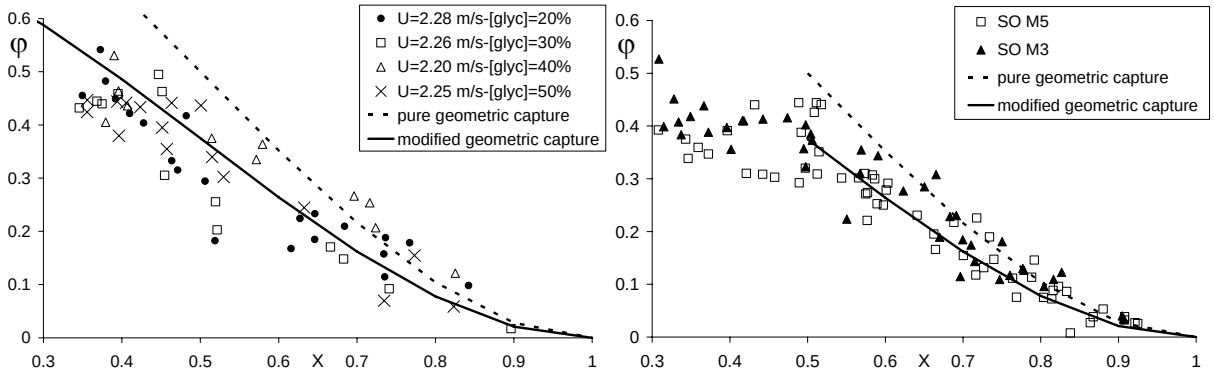

Figure 10. Left**:** Evolution of φ with X for [glyc]=50%, 40%, 30%, and 20% and SO M3, D=200 µm ±10%. Right: Evolution of φ with X for [glyc]=50% and both SO M3 and SO M5, D=200 µm ±10%.

contact, they immediately start to rotate and reduce this volume. The solid lines of Figs. 9 and 10 ("modified geometric capture"), which fit our measurements very well, correspond to 75% of the capture predicted by a "pure geometric capture". This result is very important, since it allows us to tune the thickness of the coating layer reliably and with good accuracy by simple adjustment of X for all pairs of liquids tested so far.

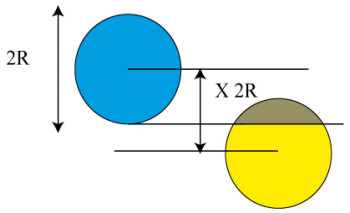

Figure 11. Interacting volume $V=(1-X)^2(1+2X)$ for $X > 0.5$. V is overestimated because of the drop rotation.

Conclusions

We presented experimental investigations on immiscible liquid droplet collisions for encapsulation. Aqueous glycerol solutions and silicon oils were tested. We described a new unstable mechanism replacing reflexive separation, which we term "crossing separation". For off-center collisions, the coating thickness scales with the impact parameter, independent of both the pair of liquids and the relative velocity of the drops. The relative velocity corresponding to the stability limit of head-on collisions scales with the viscosity of the coating liquid. Further tests will vary the interfacial tensions of the pairs of liquids.

We acknowledge financial support from the Hubert Curien Program AMADEUS 2009 from the French Ministry of Foreign Affairs and the Austrian ÖAD, and many fruitful discussions with Elise Lorenceau–Bossy at LPMDI of Université Marne-la-Vallée. We wish to thank the institute TVTUT of Graz University of Technology for support. Financial support from the Steiermärkische Landesregierung for C. Planchette is gratefully acknowledged.

References

1. Jiang, Y.J., Umemura, A., Law, C.K., *J. Fluid Mech.* 234:171-190 (1992).
2. Ashgriz, N., Poo, J.Y., *J. Fluid Mech.* 221:183-204 (1990).
3. Qian, J., Law, C. K., *J. Fluid Mech.* 331:59-80 (1997).
4. Brazier-Smith, P. R., Jennings, S.G., Latham, J., *Proc. R. Soc. Lond.* A 326:393-408 (1972).
5. Orme M., *Prog. Energy Combust. Sci.* 23: 65-79 (1997).
6. Gotaas, C., Havelka, P., Jakobsen, H.A., Svendsen, H.F., Hase, M., Roth, N., Weigand, B., *Phys. Fluids* 19:102106 (2007).
7. Brenn, G., Valkovska, D., Danov, K.D., *Phys. Fluids* 13:2463-2477 (2001).
8. Gao, T.-C., Chen, R.-H., Pu, J.-Y, Lin, T.-H., *Exp. Fluids* 38:731–738 (2005).
9. Chen, R.-H., *Applied Thermal Eng.* 27:604–610 (2007).
10. Chen, R.-H., Chen, C.-T., *Exp. Fluids* 41:453-461 (2006).
11. Dorsey, N.E., *Properties of Ordinary Water-Substance,* New York, 1940, p. 184.
12. Brenn, G., Tropea, C., Durst, F., *Part. Part. Syst. Charact.* 13:179-185 (1996).